

Revealing Fe magnetism in lanthanide-iron intermetallic compounds by tuning the rare-earth $L_{2,3}$ -edge x-ray absorption edges

M. A. Laguna-Marco,¹ J. Chaboy,^{2,*} C. Piquer,² H. Maruyama,³ N. Ishimatsu,³ N. Kawamura,⁴ M. Takagaki,⁴ and M. Suzuki⁴

¹*CITIMAC, Universidad de Cantabria, Avda. de los Castros s/n, 39005 Santander, Spain*

²*Instituto de Ciencia de Materiales de Aragón, CSIC-Universidad de Zaragoza, 50009 Zaragoza, Spain*

³*Graduate School of Science, Hiroshima University, 1-3-1 Kagamiyama, Higashi-Hiroshima 739-8526, Japan*

⁴*Japan Synchrotron Radiation Research Institute, 1-1-1 Kouto, Mikazuki, Sayo, Hyogo 679-5148, Japan*

(Received 6 July 2005; published 26 August 2005)

We present a systematic x-ray magnetic circular dichroism (XMCD) study performed at the rare-earth $L_{2,3}$ edges in $R(\text{Al}_{1-x}\text{Fe}_x)_2$ Laves phase compounds. The progressive substitution of Al by Fe reveals the existence of a non-negligible contribution of Fe to the rare-earth XMCD spectra. This contribution has been isolated and shown to be similar to the dichroic spectrum recorded at the Fe K edge. These results open the possibility of monitoring the Fe magnetism in lanthanides-iron intermetallic compounds by probing the rare-earth $L_{2,3}$ -edge x-ray absorption edges.

DOI: [10.1103/PhysRevB.72.052412](https://doi.org/10.1103/PhysRevB.72.052412)

PACS number(s): 75.50.Bb, 61.10.Ht, 78.70.Dm

Intermetallic compounds containing rare earths (R) and iron are of great technological significance owing to their industrial applications as high-performance permanent magnets. The intrinsic magnetic properties of these materials are determined by the exchange interaction between the R - $4f$ and Fe - $3d$ electrons. This interaction takes place through the hybridization of the Fe $3d$ states with the $5d$ ones of the rare earth.¹ Consequently, the study of the R - $5d$ states is of great significance to the search of new advanced magnetic materials within the R - Fe series. However, the magnetic characterization of these $5d$ states is not achieved by using standard magnetic probes. Indeed, the magnetic response of the $5d$ states to these probes is hidden by that of the localized $4f$ states. Within this framework, the experimental development²⁻⁴ of the x-ray magnetic circular dichroism (XMCD) technique^{5,6} evoked a far-reaching interest. XMCD gained popularity due to the possibility of obtaining an element-specific quantitative determination of spin and orbital magnetic moments through sum-rule analyses of experimental spectra.^{7,8} In addition, one of the most promising capabilities of XMCD concerning rare earths lies on the possibility of disentangling the magnetic contribution of the $5d$ and $4f$ states through an adequate choice of the absorption edge. Unfortunately, the XMCD expectations focused in lanthanides magnetism have not been completely fulfilled, especially regarding the magnetic probe of the $5d$ states. In principle, the characterization of the R - $5d$ states can be obtained from the XMCD spectra recorded at the $L_{2,3}$ absorption edges. However, the interpretation of the R $L_{2,3}$ -edge XMCD spectra is complicated due to two facts: (i) the contribution of quadrupolar $2p \rightarrow 4f$ transitions to the XMCD spectra is not negligible;⁹ (ii) the radial matrix elements of the dipolar $2p \rightarrow 5d$ transitions are spin dependent due to the exchange interaction between the $5d$ and the localized $4f$ orbitals.^{10,11} As a consequence, both the sign and magnitude of the XMCD signals are modified. This prevents the determination of the $5d$ magnetic moments by the simple application of the sum rules. These results led to renewed efforts

aimed to provide a proper description of the XMCD at the $L_{2,3}$ edges of the rare earths.¹²⁻¹⁶ Recent theoretical works suggest the need of including the hybridization between the R - $5d$ and Fe - $3d$ bands to account for the R - $L_{2,3}$ XMCD (Refs. 12 and 13) in the case of R - Fe intermetallics. These works are in agreement with previous claims about the contribution of the rare-earth to the Fe K -edge XMCD signal in these R - Fe compounds.¹⁷⁻¹⁹

In this Paper, we present a systematic XMCD study performed through the ferromagnetic $R(\text{Al}_{1-x}\text{Fe}_x)_2$ series^{20,21} aimed to investigate the influence of Fe on the rare-earth $L_{2,3}$ -XMCD spectra in lanthanides-iron intermetallic compounds. The progressive substitution of Al by Fe increases both the number of Fe ions surrounding the absorbing lanthanide and the strength of the $\text{Fe}(3d)$ - $R(5d)$ hybridization without modifying the crystal structure. Our results show that Fe is at the origin of well defined spectral features at the rare-earth $L_{2,3}$ edges. The contribution of Fe to the rare-earth XMCD spectra has been isolated showing a strong similarity with the Fe K -edge XMCD spectra recorded on the same compounds.

Polycrystalline $R(\text{Al}_{1-x}\text{Fe}_x)_2$ samples ($R=\text{Gd}, \text{Tb}, \text{Dy}, \text{Ho}$, and Lu) were prepared by arc melting in an argon atmosphere according to standard methods.²¹ The as-cast alloys were wrapped in Ta foil and enclosed in silica tubes, under Ar gas. Compounds were annealed at 800 °C for 72 h and then quenched to room temperature. X-ray diffraction analyses indicate that all the samples show the MgCu_2 -type ($C15$) Laves structure, with the exception of compounds with $x=0.5$ which crystallize in the hexagonal MgZn_2 -type ($C14$) structure. The presence of secondary phases is less than 5% overall, in all the cases. The cell parameters, determined from the XRD patterns, are in agreement with those previously reported.²¹ Rare-earth $L_{2,3}$ -edge XMCD experiments were performed at the beamline BL39XU of the SPring-8 facility.²² XMCD spectra were recorded in the transmission mode using the helicity-modulation technique.²³ XMCD spectra were recorded at fixed temperature $T=5$ K and under

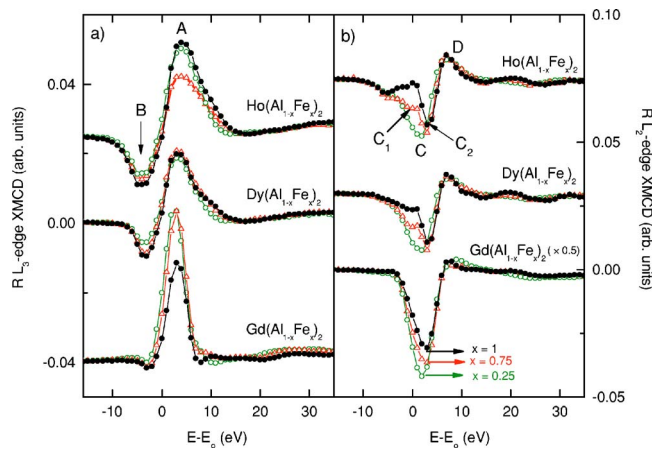


FIG. 1. (Color online) Rare-earth L_3 (a) and L_2 edge (b) XMCD ($T=5$ K, $H=50$ kOe) spectra of $R(\text{Al}_{1-x}\text{Fe}_x)_2$ compounds with $R = \text{Gd}, \text{Dy}$ and Ho : $x=1$ (\bullet), $x=0.75$ (\triangle), and $x=0.25$ (\circ). The Gd L_2 spectra are multiplied by 0.5. The labels (A to D) refer to the main spectral features that are discussed in the text. Within each panel all the signals are displayed by using the same scale and vertically shifted for sake of clarity. For both L_3 and L_2 XMCD spectra the comparison has been made in unique $E-E_0$ energy scale and no energy shift has been allowed. In every case the reference energy E_0 has been chosen at the inflection point of its corresponding absorption spectra.

the action of an applied magnetic field of 50 kOe. The spin-dependent absorption coefficient was then obtained as the difference of the XAS spectra for antiparallel and parallel orientation of the photon helicity and sample magnetization. In all the cases, the origin of the energy scale was chosen at the inflection point of the absorption edge and the XAS spectra were normalized to the averaged absorption coefficient at high energy (~ 60 eV above the edge).

The XMCD spectra recorded at the rare-earth $L_{2,3}$ edges in the $R(\text{Al}_{1-x}\text{Fe}_x)_2$ samples for $R = \text{Gd}, \text{Dy}$, and Ho are shown in Fig. 1. The spectra at the L_3 edge are dominated by a main positive peak (A) at ~ 3 eV above the edge. In the case of Dy and Ho samples there is also a negative dip (B) at energies below the edge (~ -3 eV). This latter spectral feature has been associated to a quadrupolar transition²⁴ that should be present at the L_3 edge spectra of heavy rare earths. To date, experimental evidences for the occurrence of these quadrupolar channels have been provided in the case of Dy and Er (Refs. 25 and 26) but it has never been clearly observed in the case of Gd. As shown in Fig. 1, this transition is also present in the case of Gd although its intensity is significantly reduced when compared to that of heavier rare-earths as Dy or Ho. Upon substitution of Al by Fe the shape of the L_3 XMCD spectra is mostly retained through the whole $R(\text{Al}_{1-x}\text{Fe}_x)_2$ series. The modification of the intensity of the main XMCD spectral features (A and B) as a function of the Fe content depends on the rare earth. In all the cases peak B is enhanced by increasing the Fe content. However, no uniform variation is observed regarding the A-peak intensity. The peculiar behavior of the spectral features induced by the Fe—Al substitution is also observed at the L_2 XMCD signals. As shown in Fig. 1 the spectral profile of the L_2 -edge

spectra consists of a main negative peak (C) centered at ~ 3 eV above the edge and a positive peak (D) at higher, ~ 7 eV, energy. In the case of the $\text{Gd}(\text{Al}_{1-x}\text{Fe}_x)_2$ compounds, the spectral shape remains unaffected by the Fe substitution. However, as the Fe content increases the intensity of the main peak C decreases by a $\sim 40\%$ as going from $\text{Gd}(\text{Al}_{0.75}\text{Fe}_{0.25})_2$ to GdFe_2 . By contrast, the Dy and Ho compounds exhibit a quite different behavior. The L_2 -edge XMCD spectra of the Al-rich compounds show a main negative peak as in the case of the Gd compounds. However, as the Fe content increases in the material the negative C peak starts to split in two components C_1 and C_2 (see Fig. 1). The depletion of the low-energy (C_1) component is progressive as the iron content increases, whereas the modification of the intensity of the high-energy (C_2) component is less marked. As discussed above, the Gd L_2 -edge XMCD spectra of the $\text{Gd}(\text{Al}_{1-x}\text{Fe}_x)_2$ compounds do not show the splitting of the C_1 and C_2 structures. However, the position of the minimum is shifted (~ 1 eV) towards higher energy and its intensity decreases. In the case of GdFe_2 this intensity is $\sim 25\%$ smaller than for the $\text{Gd}(\text{Al}_{0.75}\text{Fe}_{0.25})_2$ compound. These results suggest that although C_1 and C_2 structures cannot be energy resolved the low-energy component of the C peak is also pushed up in the $\text{Gd}(\text{Al}_{1-x}\text{Fe}_x)_2$ series by increasing the Fe content.

These results point out the existence of an extra contribution at the rare-earth L_2 -edge XMCD spectra through the whole $R(\text{Al}_{1-x}\text{Fe}_x)_2$ series that is connected to the presence of Fe. The magnetic characterization conducted at the macroscopic level indicates that neither the electronic nor the magnetic state of the rare-earth atoms are modified upon substitution of Al by Fe through the whole $R(\text{Al}_{1-x}\text{Fe}_x)_2$ series. Consequently, the observed behavior cannot be associated to the modification of the quadrupolar transitions as they involve the $4f$ states which are unaffected by the Fe—Al substitution. On the contrary, these results suggest that the origin of the peculiar modification of the spectral intensities, showing emerging features, is related to the number of magnetic Fe atoms in the neighborhood of the rare-earth one.

The contribution of the $5d$ - $3d$ exchange to the rare-earth L_3 -edge XMCD signals was early suggested by Lang *et al.*²⁷ This hypothesis is in agreement with previous XMCD works performed at the Fe K edge in several R -Fe intermetallics showing that there is a contribution coming from the rare earth even when the Fe is probed.^{17–19} Therefore, the present results, showing the Fe contribution to the rare-earth $L_{2,3}$ edges XMCD spectra are the counterpart of the detected lanthanide contribution to the Fe K edge in R -Fe intermetallics. Aimed to demonstrate this assumption we have isolated the Fe contribution to the lanthanide XMCD signals in the following way: for a given R we have subtracted to the L_2 XMCD spectra of the $R(\text{Al}_{1-x}\text{Fe}_x)_2$ compounds the XMCD signal of the compound with the lowest Fe content. In order to maintain the same experimental conditions we have subtracted the Tb L_2 XMCD signals recorded in TbAl_2 to that of the $\text{Tb}(\text{Al}_{1-x}\text{Fe}_x)_2$ compounds, while the XMCD signal of the $\text{R}(\text{Al}_{0.75}\text{Fe}_{0.25})_2$ compound was subtracted in the case of $R = \text{Gd}, \text{Dy}$, and Ho . As shown in Fig. 2, the extracted signal consists on an intense positive peak at the edge followed by

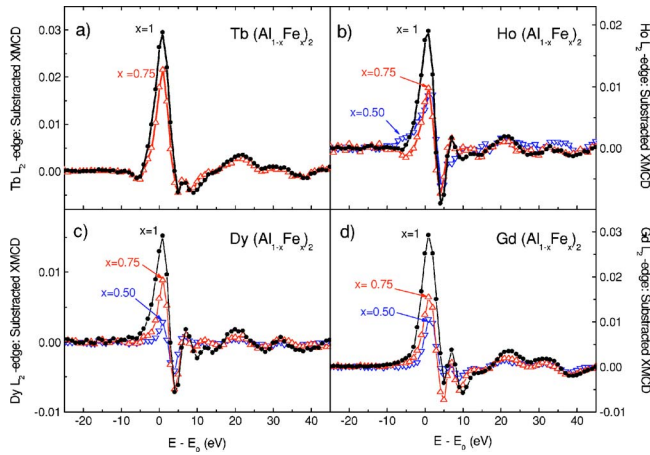


FIG. 2. (Color online) Rare-earth L_2 -edge XMCD ($T=5$ K, $H=50$ kOe) spectra of the $R(\text{Al}_{1-x}\text{Fe}_x)_2$ compounds with $x=1$ (\bullet), 0.75 (Δ), and 0.5 (∇), after subtracting the XMCD spectrum of the compound with the lowest Fe content: $R=\text{Tb}$ (a), Ho (b), Dy (c), and Gd (d). The subtraction and the comparison have been performed in a unique $E-E_0$ energy scale. For every compound the reference energy E_0 has been chosen at the inflection point of the absorption spectra.

an smaller double negative peak at higher energies. The spectral shape is the same no matter the rare earth. The profile of the isolated signals is also kept invariable with Fe content and only the relative intensity of the different spectral features changes with the Fe content. In all the studied cases the intensity of the signal extracted by using the above procedure increases with the Fe content, i.e., with the number of Fe atoms surrounding the absorbing lanthanide ion. These results suggest that the extracted signals correspond to a magnetic contribution of Fe atoms to the rare-earth L edges XMCD.

Finally, the extracted signals have been compared to the Fe K -edge XMCD spectra of both LuFe_2 and pure iron. The comparison, shown in Fig. 3, has been made in a unique energy scale, i.e., the E_0 at the Fe K edge was also chosen at the inflection point of the absorption edge. It should be stressed that no energy shift was applied between both the extracted L_2 signal and the Fe K -edge XMCD spectra. As shown in Fig. 3 the similarity between the signals is remarkable, supporting our initial hypothesis about the contribution of Fe atoms to the rare-earth L_2 XMCD. In particular, both the difference L_2 signal and the Fe K -edge XMCD spectrum of LuFe_2 exhibit a positive peak (P_1) at the absorption edge, and both a negative (P_2), and positive (P_3) peaks at ~ 4 and 7 eV above the edge, respectively. By contrast, this double spectral feature is absent in the case of the Fe K -edge XMCD spectrum of pure iron. These results showing the agreement between the extracted signal from the L_2 XMCD spectra and the Fe K edge of LuFe_2 , i.e., of a compound with the same

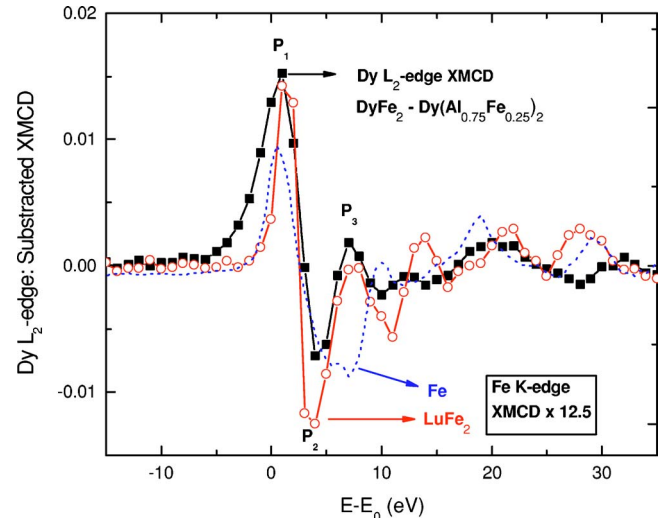


FIG. 3. (Color online) Comparison between the Fe K -edge XMCD spectrum of LuFe_2 (\circ) and pure Fe (dotted line) compounds and the signal obtained by subtracting the Dy L_2 -edge XMCD spectrum of $\text{Dy}(\text{Al}_{0.75}\text{Fe}_{0.25})_2$ to that of DyFe_2 . The Fe K -edge XMCD spectra are multiplied by a 12.5 factor. The comparison is displayed on a unique $E-E_0$ energy scale. For each Dy L_2 and Fe K -edge XMCD spectrum, E_0 has been chosen at the inflection point of its corresponding absorption spectra.

crystal structure and only Fe magnetism, supports our hypothesis of the magnetic contribution of Fe atoms to the L -edge XMCD spectra of the rare earths.

Summarizing, we have presented a systematic XMCD study at the rare-earth $L_{2,3}$ edges in $R(\text{Al}_{1-x}\text{Fe}_x)_2$ compounds. The evolution of the L_2 dichroic signal from Al-rich $R(\text{Al}_{1-x}\text{Fe}_x)_2$ compounds to $R\text{Fe}_2$ points out the presence of a magnetic contribution from the surrounding Fe atoms. This contribution has been isolated from the spectra and shown to resemble the Fe K -edge XMCD signal of LuFe_2 . These results suggest that this contribution arises from the $R(5d)$ - $\text{Fe}(3d)$ hybridization although further work is in progress to determine the exact nature of this contribution. These experimental findings indicate the need of including an iron contribution prior to account for the XMCD at the rare-earth $L_{2,3}$ edges in R -Fe intermetallic materials and, consequently, of getting the characterization of the lanthanides $5d$ states by means of XMCD. In addition, these results open the possibility of monitoring the Fe magnetism in lanthanides-iron intermetallic compounds by probing the rare-earth $L_{2,3}$ -edge x-ray absorption edges.

This work was partially supported by the Spanish CICYT-MAT2002-04178-C04-03 grant. The synchrotron radiation experiments were performed at SPring-8 (Proposal Nos. 2003A0118-NS2-np and 2003B0064-NSc-np).

*Corresponding author.

- ¹I. A. Campbell, *J. Phys. F: Met. Phys.* **2**, L47 (1972).
- ²E. Keller and E. A. Stern, in *EXAFS and Near Edge Structure III*, edited by K. O. Hodgson, B. Hedman, and J. E. Penner-Hahn (Springer-Verlag, Heidelberg, 1984), p. 507.
- ³G. Schütz, W. Wagner, W. Wilhelm, P. Kienle, R. Zeller, R. Frahm, and G. Materlik, *Phys. Rev. Lett.* **58**, 737 (1987).
- ⁴G. van der Laan, B. T. Thole, G. A. Sawatzky, J. B. Goedkoop, J. C. Fuggle, J.-M. Esteva, R. Karnatak, J. P. Remeika, and H. A. Dabkowska, *Phys. Rev. B* **34**, 6529 (1986).
- ⁵J. L. Erskine and E. A. Stern, *Phys. Rev. B* **12**, 5016 (1975).
- ⁶B. T. Thole, G. van der Laan, and G. A. Sawatzky, *Phys. Rev. Lett.* **55**, 2086 (1985).
- ⁷B. T. Thole, P. Carra, F. Sette, and G. van der Laan, *Phys. Rev. Lett.* **68**, 1943 (1992).
- ⁸P. Carra, B. T. Thole, M. Altarelli, and X. Wang, *Phys. Rev. Lett.* **70**, 694 (1993).
- ⁹P. Carra, B. N. Harmon, B. T. Thole, M. Altarelli, and G. A. Sawatzky, *Phys. Rev. Lett.* **66**, 2495 (1991).
- ¹⁰B. N. Harmon and A. J. Freeman, *Phys. Rev. B* **10**, 1979 (1974); **10**, 4849 (1974).
- ¹¹X. Wang, T. C. Leung, B. N. Harmon, and P. Carra, *Phys. Rev. B* **47**, 9087 (1993).
- ¹²K. Fukui, H. Ogasawara, A. Kotani, I. Harada, H. Maruyama, N. Kawamura, K. Kobayashi, J. Chaboy, and A. Marcelli, *Phys. Rev. B* **64**, 104405 (2001).
- ¹³K. Asakura, J. Nakahara, I. Harada, H. Ogasawara, K. Fukui, and A. Kotani, *J. Phys. Soc. Jpn.* **71**, 2771 (2002).
- ¹⁴H. Wende, Z. Li, A. Scherz, G. Ceballos, K. Baberschke, A. Ankudinov, J. J. Rehr, F. Wilhelm, A. Rogalev, D. L. Schlagel, and T. A. Lograsso, *J. Appl. Phys.* **91**, 7361 (2002).
- ¹⁵J. Chaboy, H. Maruyama, N. Kawamura, and M. Suzuki, *Phys. Rev. B* **69**, 014427 (2004).
- ¹⁶C. Giorgetti, E. Dartyge, F. Baudelet, and R.-M. Galera, *Phys. Rev. B* **70**, 035105 (2004).
- ¹⁷J. Chaboy, H. Maruyama, L. M. García, J. Bartolomé, K. Kobayashi, N. Kawamura, A. Marcelli, and L. Bozukov, *Phys. Rev. B* **54**, R15637 (1996).
- ¹⁸J. Chaboy, L. M. García, F. Bartolomé, H. Maruyama, S. Uemura, N. Kawamura, and A. S. Markosyan, *J. Appl. Phys.* **88**, 1 (2000).
- ¹⁹J. Chaboy, M. A. Laguna-Marco, M. C. Sanchez, H. Maruyama, N. Kawamura, and M. Suzuki, *Phys. Rev. B* **69**, 134421 (2004).
- ²⁰W. Steiner, *J. Magn. Magn. Mater.* **14**, 47 (1979).
- ²¹See, for example, V. Sima *et al.*, *J. Phys. F: Met. Phys.* **14**, 981 (1984), and references therein.
- ²²H. Maruyama, M. Suzuki, N. Kawamura, M. Ito, E. Arakawa, J. Kokubun, K. Hirano, K. Horie, S. Uemura, K. Hagiwara, M. Mizumaki, S. Goto, H. Kitamura, K. Namikawa, and T. Ishikawa, *J. Synchrotron Radiat.* **6**, 1133 (1999).
- ²³M. Suzuki, N. Kawamura, M. Mizumaki, A. Urata, H. Maruyama, S. Goto, and T. Ishikawa, *Jpn. J. Appl. Phys., Part 2* **37**, L1488 (1998).
- ²⁴F. Bartolomé, J. M. Tonnerre, L. Seve, D. Raoux, J. Chaboy, L. M. García, M. Krisch, and C. C. Kao, *Phys. Rev. Lett.* **79**, 3775 (1997).
- ²⁵J. C. Lang, G. Srajer, C. Detlefs, A. I. Goldman, H. König, X. Wang, B. N. Harmon, and R. W. McCallum, *Phys. Rev. Lett.* **74**, 4935 (1995).
- ²⁶J. C. Lang, S. W. Kycia, X. Wang, B. N. Harmon, A. I. Goldman, D. J. Branagan, R. W. McCallum, and K. D. Finkelstein, *Phys. Rev. B* **46**, 5298 (1992).
- ²⁷J. C. Lang, G. Srajer, C. S. Nelson, C. T. Venkataramen, A. I. Goldman, C. Detlets, Z. Islam, B. N. Harmon, K. W. Dennis, and R. W. McCallum (unpublished).